



# An iminocoumarin benzothiazole-based fluorescent probe for imaging hydrogen sulfide in living cells



Huatang Zhang<sup>a</sup>, Yusheng Xie<sup>a</sup>, Ping Wang<sup>a</sup>, Ganchao Chen<sup>a</sup>, Ruochuan Liu<sup>a</sup>, Yun-Wah Lam<sup>a</sup>, Yi Hu<sup>b</sup>, Qing Zhu<sup>c,\*</sup>, Hongyan Sun<sup>a,\*</sup>

<sup>a</sup> Department of Biology and Chemistry, City University of Hong Kong, 83 Tat Chee Avenue, Kowloon, Hong Kong, China

<sup>b</sup> CAS Key Laboratory for Biomedical Effects of Nanomaterials and Nanosafety, CAS Key Lab of Nuclear Radiation and Nuclear Energy Technology, Center for Multidisciplinary Research, Institute of High Energy Physics, Chinese Academy of Sciences (CAS), Beijing 100049, China

<sup>c</sup> Institute of Bioengineering, Zhejiang University of Technology, Chaowang Road 18, Hangzhou 310014, China

## ARTICLE INFO

### Article history:

Received 31 October 2014

Received in revised form

24 December 2014

Accepted 27 December 2014

Available online 6 January 2015

### Keywords:

Fluorescent probe

Hydrogen sulfide

Cell imaging

Iminocoumarin benzothiazole

## ABSTRACT

Hydrogen sulfide (H<sub>2</sub>S) has recently been identified as the third gaseous signaling molecule that is involved in regulating many important cellular processes. We report herein a novel fluorescent probe for detecting H<sub>2</sub>S based on iminocoumarin benzothiazole scaffold. The probe displayed high sensitivity and around 80-fold increment in fluorescence signal after reacting with H<sub>2</sub>S under physiological condition. The fluorescent intensity of the probe was linearly related to H<sub>2</sub>S concentration in the range of 0–100 μM with a detection limit of 0.15 μM (3σ/slope). The probe also showed excellent selectivity towards H<sub>2</sub>S over other biologically relevant species, including ROS, RSS and RNS. Its selectivity for H<sub>2</sub>S is 32 folds higher than other reactive sulfur species. Furthermore, the probe has been applied for imaging H<sub>2</sub>S in living cells. Cell imaging experiments demonstrated that the probe is cell-permeable and can be used to monitor the alteration of H<sub>2</sub>S concentrations in living cells. We envisage that this probe can provide useful tools to further elucidate the biological roles of H<sub>2</sub>S.

© 2015 Elsevier B.V. All rights reserved.

## 1. Introduction

Hydrogen sulfide (H<sub>2</sub>S) has recently emerged as the third gaseous signaling molecule after carbon monoxide and nitric oxide [1]. Recent biological studies have established the important role of H<sub>2</sub>S in various physiological and pathological processes [2–6]. For example, H<sub>2</sub>S has been shown to regulate inflammation, relax smooth muscles and act as a vasodilator. It has strong implications in neurodegeneration, and studies have shown that it might be able to protect neurons from secondary neuronal injuries through multiple biological mechanisms, such as anti-oxidation and anti-apoptosis [7]. In mammalian cells, H<sub>2</sub>S can be produced through both enzymatic and non-enzymatic biosynthesis. In enzymatic biosynthesis, cysteine or its derivatives can be converted to H<sub>2</sub>S through the catalysis of several enzymes, such as cystathionine γ-lyase (CSE), cystathionine β-synthase (CBS), cysteine aminotransferase (CAT) and 3-mercaptopyruvate sulfurtransferase (MST) [8–10]. On the other hand, glutathione and polysulfides can be transformed to H<sub>2</sub>S through

non-enzymatic pathway [11,12]. Increasing evidence has shown that abnormal levels of H<sub>2</sub>S is closely linked to several important diseases, such as Alzheimer's disease, Down's syndrome, diabetes and liver cirrhosis [13–15]. For example, it was observed that the concentrations of H<sub>2</sub>S are severely decreased in the brains of Alzheimer's disease patients compared with those in the brains of healthy individuals. In recent years, it has spurred substantial interest in scientific community to develop useful chemical tools to accurately measure H<sub>2</sub>S levels in biological systems.

Till date, many different methods have been developed for detecting H<sub>2</sub>S, including electrochemical methods, colorimetric methods, gas chromatography and polarographic sensors [16–21]. Among these methods, fluorescence-based methods have attracted intensive interest due to their highly sensitive and non-invasive properties. In addition, fluorescence-based methods also allow one to monitor the molecules of interest in a native environment, thereby providing detailed spatial and kinetic information. Since the first H<sub>2</sub>S probe was reported in 2011, a number of H<sub>2</sub>S fluorescent probes have been designed and applied to imaging H<sub>2</sub>S in live cells. These fluorescent probes can be mainly categorized into three types. 1) Probes containing an azide/nitro group that can effectively quench fluorescence [22–30]. When H<sub>2</sub>S reduces the azide/nitro group, fluorescence will be turned on. 2) Probes that utilize the double

\* Corresponding author. Tel.: +852 34429537; fax: +852 34420522.

\*\* Corresponding author. Tel.: +86 571 88320781; fax: +86 571 88320781.

E-mail addresses: [zhuq@zjut.edu.cn](mailto:zhuq@zjut.edu.cn) (Q. Zhu), [hongyansun@cityu.edu.hk](mailto:hongyansun@cityu.edu.hk) (H. Sun).

nucleophilicity property of H<sub>2</sub>S to switch on fluorescence [31–34]. 3) Probes containing a chelating unit that forms complex with Cu<sup>2+</sup> [35–37]. Addition of H<sub>2</sub>S can release Cu<sup>2+</sup>, leading to fluorescence enhancement.

Biological research on H<sub>2</sub>S has been carried out intensively by the scientific community. Notwithstanding, the production process, tissue specificity and action mechanism of H<sub>2</sub>S still need to be further elucidated. We envisage that H<sub>2</sub>S fluorescent probe with innovative design, high kinetics and improved fluorescent property will be highly useful to further elucidate the biological roles of H<sub>2</sub>S.

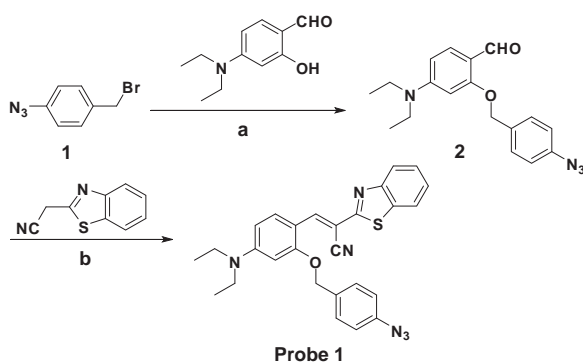
Inspired by the work of Kim's team [38], we designed and synthesized a new fluorescent probe 1 based on iminocoumarin benzothiazole to detect H<sub>2</sub>S. The iminocoumarin-based fluorophore has been proven to possess excellent photophysical properties, such as good photostability and high quantum yield. In addition, our probe can be excited at long wavelength (465 nm). Compared with probes used under short wavelength irradiation, our probe can minimize cell damage and is more suitable for bioimaging studies. Furthermore, the probe has high signal-to-noise ratio, which is attributed to its special chemical structure. The probe itself has little fluorescence due to fast non-radioactive decay of the singlet excited state through internal bond rotations [39]. Upon reacting with H<sub>2</sub>S, it will form a cyclized iminocoumarin benzothiazole structure that is highly fluorescent.

Probe 1 was synthesized through the following synthetic route (Scheme 1). *P*-azidebenzyl linker 1 was first prepared according to published procedure. It was then used to react with the free phenol hydroxyl group of 4-(diethylamino) salicylaldehyde under refluxing condition. The resulting compound 2 was subsequently subjected to Knoevenagel condensation with 2-benzothiazoleacetonitrile to afford the final probe 1. The structures of probe 1 and the synthetic intermediates were all characterized by <sup>1</sup>H NMR, <sup>13</sup>C NMR and ESI-MS respectively (supporting Information).

## 2. Experimental details

### 2.1. Apparatus

<sup>1</sup>H NMR and <sup>13</sup>C NMR spectrums were recorded on a Bruker 400 MHz NMR spectrometer. Fluorescence emission spectra were obtained with FluoroMax-4 fluorescence photometer. UV absorption spectra were obtained on Shimadzu 1700 UV/Vis Spectrometer. Mass spectra were obtained using a PC Sciex API 150 EX ESI-MS system. Fluorescence images were acquired with a Leica TCS SPE Confocal Scanning Microscope. pH value was recorded with a FiveEasy™ Fe20 pH meter.



**Scheme 1.** Synthetic route of probe 1.a) K<sub>2</sub>CO<sub>3</sub>, acetone, reflux, 3 h, 78%; b) Piperidine, EtOH, rt, 5 h, 80%.

### 2.2. Reagents

4-aminobenzylalcohol, 4-(diethylamino)salicylaldehyde, sodium nitrite and sodium azide were purchased from Acros. Tribromophosphane, piperidine and 2-(1,3-benzothiazol-2-yl)acetonitrile were obtained from J&K Chemical. Dulbecco's modified Eagle's medium (DMEM), PBS, fetal bovine serum (FBS), trypsin-EDTA and penicillin/streptomycin were purchased from Invitrogen. Other reagents were all of analytical grade and were used without further purification. Milli-Q water was used in all experiments.

### 2.3. Synthesis of 1-azido-4-(bromomethyl)benzene (1)

1-azido-4-(bromomethyl) benzene was synthesized according to literature. Details of synthesis are shown in Scheme S1 (Supporting Information).

### 2.4. Synthesis of 2-((4-azidobenzyl)oxy)-4-(diethylamino)benzaldehyde (2)

4-(Diethylamino)salicylaldehyde (0.096 g, 0.50 mmol), K<sub>2</sub>CO<sub>3</sub> (0.138 g, 1.00 mmol) and 1-azido-4-(bromomethyl)benzene (0.084 g, 0.40 mmol) were dissolved in dry acetone (5.0 mL) under nitrogen atmosphere. The mixture was stirred at 60 °C for 3 h. After filtration, the solvent was evaporated under reduced pressure. The crude product was purified by silica gel column chromatography with hexane/ethyl acetate=3/1 to obtain compound 2 as a yellow solid (0.100 g, 77.2% yield); <sup>1</sup>H NMR (400 MHz, CDCl<sub>3</sub>): δ= 10.19 (s, 1H), 7.70 (d, *J*=8.0 Hz, 1H), 7.41 (d, *J*=8.0 Hz, 2H), 7.01 (d, *J*=8.0 Hz, 2H), 6.27 (d, *J*=8.0 Hz, 1H), 6.03 (s, 1H), 5.10 (s, 2H), 3.36 (q, 4H), 1.15 (t, 6H); <sup>13</sup>C NMR (100 MHz, CDCl<sub>3</sub>): δ= 186.8, 163.0, 153.7, 139.8, 133.3, 130.5, 128.7, 119.2, 114.3, 104.6, 94.0, 69.5, 44.8, 12.5; ESI-MS: calcd. for C<sub>18</sub>H<sub>21</sub>N<sub>4</sub>O [M+H]<sup>+</sup> 325.2; found, 325.4.

### 2.5. Synthesis of probe 1

One drop of piperidine was added to a stirred solution of 2 (0.097 g, 0.30 mmol) and 2-(1,3-benzothiazol-2-yl)acetonitrile (0.052 g, 0.30 mmol) in ethanol (5.0 mL) under nitrogen atmosphere at room temperature. The reaction mixture was stirred for 5 h at room temperature. The solvent was evaporated under reduced pressure. The crude product was purified by silica gel column chromatography with hexane/ethyl acetate=5/1 to obtain the probe 1 as a red solid (0.115 g, 79.9%). <sup>1</sup>H NMR (400 MHz, CDCl<sub>3</sub>): δ=8.60 (s, 1H), 8.44 (d, *J*=8.0 Hz, 1H), 8.02 (d, *J*=8.0 Hz, 1H), 7.84 (d, *J*=8.0 Hz, 1H), 7.47 (m, 3H), 7.35 (t, 1H), 7.08 (m, 2H), 6.43 (d, *J*=8.0 Hz, 1H), 6.18 (s, 1H), 5.18 (s, 2H), 3.40 (q, 4H), 1.18 (t, 6H); <sup>13</sup>C NMR (100 MHz, CDCl<sub>3</sub>): δ=165.8, 160.3, 154.0, 152.5, 141.1, 140.0, 134.4, 133.4, 130.6, 128.7, 126.5, 125.0, 123.0, 121.4, 119.4, 118.6, 110.2, 105.6, 96.7, 95.1, 70.1, 45.1, 12.7; ESI-MS: calcd. for C<sub>27</sub>H<sub>24</sub>N<sub>6</sub>OS [M+H]<sup>+</sup> 481.2; found, 481.4.

### 2.6. Procedure of fluorescence measurement

Probe 1 stock was diluted in Tris buffer (50 mM, pH=8.0, 50% DMF) to a final concentration of 5 μM. For the selectivity experiment, 50 mM of biologically relevant analytes were prepared as stock solutions in PBS buffer. Appropriate amounts of biologically relevant analytes were mixed thoroughly with 5 μM of Probe 1 and then incubated at 37 °C for 60 min. For the time course experiment with Na<sub>2</sub>S, 100 μM of Na<sub>2</sub>S was incubated with 5 μM of probe 1 in Tris buffer at 37 °C, and the fluorescence intensity was measured at different time points. Fluorescence emission spectra were collected using a FluoroMax-4 fluorescence photometer with a 10 mm quartz cuvette. The excitation wavelength was set to

465 nm and the emission wavelength was set in the range of 480 nm to 650 nm. The slit width was set to 5 nm.

### 2.7. Cell culture and fluorescence microscope imaging

HeLa cells were cultured in Dulbecco's modified Eagle's medium (DMEM) supplemented with 10% fetal bovine serum (FBS) and recommended working concentrations of antibiotics (penicillin and streptomycin). Approximately  $10^5$  cells were seeded in a confocal dish (35 mm). After 24 h, the cells were treated with probe 1 ( $5 \mu\text{M}$ ) at  $37^\circ\text{C}$  for 30 min and then incubated with  $\text{Na}_2\text{S}$  for another 30 min. Cells treated with probe 1 ( $5 \mu\text{M}$ ) alone were used as a control. Fluorescence images were then taken using a Leica TCS SPE Confocal Scanning Microscope.

## 3. Results and discussion

### 3.1. Proposed mechanism

Based on the mechanism of several azide-containing probes, we propose the following mechanism whereby probe 1 reacts with  $\text{H}_2\text{S}$ . First, the benzyl azide group is reduced to benzyl amine group by  $\text{H}_2\text{S}$ . The resulting *p*-aminobenzyl moiety is unstable and can undergo self-immolation through 1,6-elimination. After self-elimination of the linker, the hydroxyl group is released. It will then undergo intramolecular cyclization to yield an iminocoumarin-benzothiazole molecule, resulting in a highly conjugated structure. This cyclized iminocoumarin-benzothiazole displays significant fluorescence enhancement compared with its unreduced form (Scheme 2).

To confirm our proposed mechanism, probe 1 ( $50 \mu\text{M}$ ) and  $\text{Na}_2\text{S}$  ( $1 \text{ mM}$ ) were incubated in Tris buffer ( $50 \text{ mM}$ ,  $\text{pH}=8.0$ ,  $50\% \text{ DMF}$ ) at  $37^\circ\text{C}$ . The resulting solution was then monitored using ESI-MS. After incubating for 20 min, three peaks at  $m/z$  481.3, 350.2 and 106.3 were observed, which corresponds to the molecular weight of probe 1, iminocoumarin-benzothiazole molecule and 1,6-eliminated product respectively (Fig. S1a, Supporting Information). The peak of  $m/z$  481.3, which belongs to probe 1, could not be observed after 60 min of incubation, indicating the reaction has completed (Fig. S1b, Supporting Information).

### 3.2. UV-vis absorption and fluorescence emission of probe 1

Next we investigated the optical properties of probe 1 in the absence and the presence of  $\text{H}_2\text{S}$  ( $100 \mu\text{M}$ , using  $\text{Na}_2\text{S}$  as an equivalent). Probe 1 exhibited a maximum absorbance at 455 nm. After reacting with  $\text{H}_2\text{S}$ , the maximum absorbance was shifted to 465 nm, an increase of 10 nm (Fig. 1a). For the fluorescence emission spectrum, probe 1 showed very weak fluorescence intensity when excited at 465 nm. After reacting with  $\text{Na}_2\text{S}$ , however, probe 1 displayed strong fluorescence at 520 nm (Fig. 1b, Fig. S2, Supporting Information).

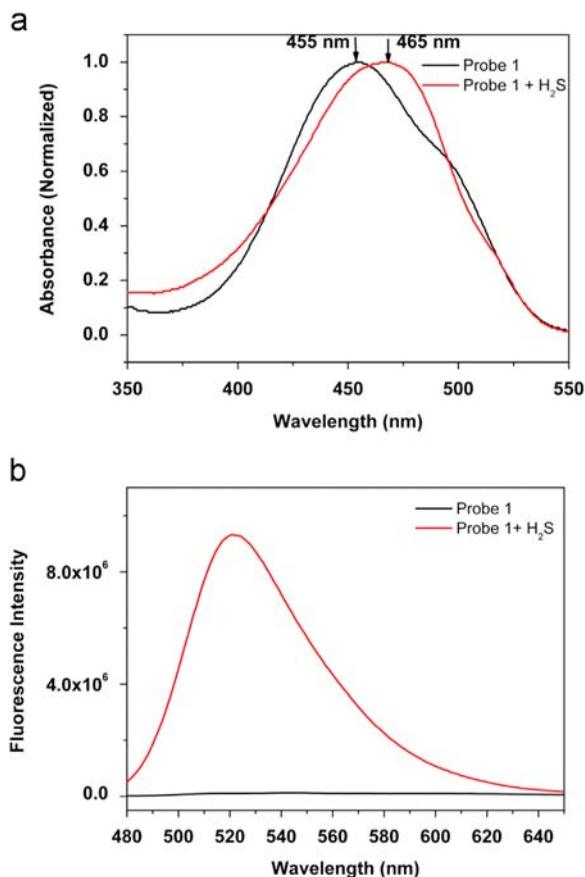


Fig. 1. (a) Absorption and (b) emission spectrum of probe 1 ( $10 \mu\text{M}$ ) in the absence and the presence of  $\text{Na}_2\text{S}$  ( $100 \mu\text{M}$ ) at  $37^\circ\text{C}$  for 60 min.

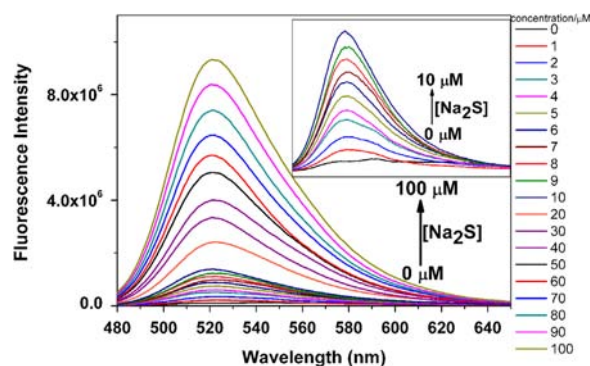
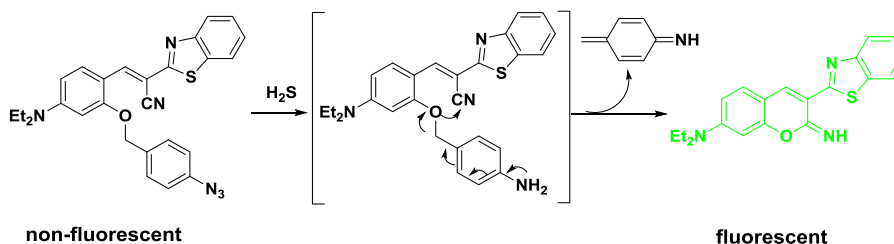


Fig. 2. Fluorescence response of probe 1 ( $5 \mu\text{M}$ ) in Tris buffer ( $50 \text{ mM}$ ,  $\text{pH}=8.0$ ,  $50\% \text{ DMF}$ ) with addition of increasing concentrations of  $\text{Na}_2\text{S}$  ( $0, 1, 2, 3, 4, 5, 6, 7, 8, 9, 10, 20, 30, 40, 50, 60, 70, 80, 90$ , and  $100 \mu\text{M}$ ),  $\lambda_{\text{ex}}=465 \text{ nm}$ ,  $\lambda_{\text{em}}=480\text{--}650 \text{ nm}$ ) after 1 h incubation at  $37^\circ\text{C}$ . The inset figure shows that the fluorescence signal increases linearly with increasing concentrations of  $\text{Na}_2\text{S}$  when the concentration is between  $0\text{--}10 \mu\text{M}$ .



Scheme 2. Proposed "turn-on" mechanism of the probe reacting with  $\text{H}_2\text{S}$ .

### 3.3. Sensitivity and detection limit

We next carried out detailed study to examine the sensitivity of probe 1 towards H<sub>2</sub>S. Fig. 2 showed the fluorescence response of probe 1 when different concentrations of Na<sub>2</sub>S (0–100 μM) were added. Approximately 80-fold increase in fluorescence intensity at 520 nm could be observed when the reaction between probe 1 and Na<sub>2</sub>S was complete. Further data analysis revealed an excellent linear relationship ( $R^2=0.99748$ ) between the fluorescent signal at 520 nm and Na<sub>2</sub>S concentrations in the range of 0 to 100 μM (Fig. S3 and S4, Supporting Information). The detection limit of probe 1 was determined to be 0.15 μM (based on the equation of  $3\sigma/m$ , where  $m$  is the slope of fluorescence intensity against Na<sub>2</sub>S concentration and  $\sigma$  is the relative standard deviation of the blank measurements) [40–42]. This value is comparable with the detection limits of other H<sub>2</sub>S probes (Table 1.). Taken together, these data prove that the new probe described here can serve as a highly sensitive sensor to detect H<sub>2</sub>S in a quantitative manner.

### 3.4. Kinetics

Subsequently we examined the reaction kinetics of probe 1 and Na<sub>2</sub>S. Probe 1 (5 μM) was incubated with Na<sub>2</sub>S (100 μM) at 37 °C in Tris-HCl buffer (50 mM, pH=8.0, 50 % DMF). The fluorescence intensity at 520 nm was recorded and plotted as a function of time for data analysis. As shown in Fig. 3, the fluorescence intensity increased rapidly at the beginning and plateaued after around

**Table 1**  
The summary of recently developed H<sub>2</sub>S probes.

Probe	$\lambda_{ex}$ (nm)	$\lambda_{em}$ (nm)	Linear range (μM)	pH condition	LOD (μM)	Increased fold	Ref.
SF1	490	525	~	7.4	5–10	7-fold	[22]
DNS- Az	340	535	5–100	7.4	1	40-fold	[23]
HSN2	432	542	~	7.4	1–5	60-fold	[24]
1	535	620	1–40	7.4	0.1	30-fold	[27]
Probe 1	465	515	0–10	7.4	1–10	55–70- fold	[31]
HSip- 1	491	516	~	7.4	10	50-fold	[35]
Cy-N3	625	750	0–100	7.4	0.08	3.3-fold	[43]
L1Cu	495	534	~	7.2	5	4-fold	[44]
NHS1	360	480	5–10	7.4	0.1	67-fold	[45]
1	520	670	25–250	7.4	3.05	65-fold	[46]
C-7Az	340	445	0.25–100	7.4	~	108-fold	[47]
1	465	520	1–100	8.0	0.15	80-fold	This work

Note: ~ means not mentioned.

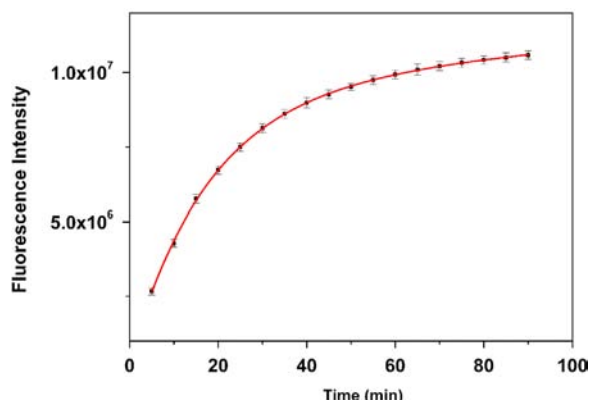


**Fig. 3.** Time course experiment of probe 1 (5 μM) reacting with Na<sub>2</sub>S (100 μM) in Tris buffer (50 mM, pH=8.0, 50% DMF) at 37 °C.

60 min. The pseudo-first-order rate constant of the reaction was calculated as  $k_{obs}=8.5 \times 10^{-4} \text{ s}^{-1}$  by fitting the fluorescence intensity data into the following equation:  $\ln(F_{max}-F_t)=\ln F_{max}-k_{obs} \times t$ . The reaction rate ( $k_2$ ) was found to be  $8.50 \text{ M}^{-1} \text{ s}^{-1}$ , which is similar to other azide-based probes reported previously.

### 3.5. Selectivity

Selectivity test is a critical step to ensure that our probe will not be interfered by other biomolecules in the complex biological system. To perform the selectivity test, various biologically relevant analytes, including reactive oxygen species (ROS), reactive nitrogen species (RNS), reactive sulfur species (RSS) and other reactive anions (Fig. 4, Fig. S5, S6, Supporting Information) were examined under the following assay conditions: different biologically relevant analytes (1 mM) were added respectively to a solution containing 5 μM of probe 1 (100 μM of Na<sub>2</sub>S was incorporated as a control). The fluorescence was measured after 60 min of incubation. As shown in Figs. 4 and S6, all the biologically relevant analytes tested did not show any obvious fluorescence increase except cysteine (2.6 fold) and I<sup>-</sup> (2.4 fold). The selectivity ratio towards Na<sub>2</sub>S over cysteine is as high as 31-fold. The excellent selectivity of probe 1 towards Na<sub>2</sub>S over other analytes suggests that probe 1 is a promising tool for specifically detecting H<sub>2</sub>S in a complex biological environment.

### 3.6. Bioimaging application in living cells

For the bioimaging applications of the probe, we first performed MTT assay to examine whether the probe is cytotoxic to cells. Results indicated that 5 μM of probe 1 did not show any significant cytotoxicity after 24 h (Fig. S7, Supporting Information). We then moved on to carry out imaging experiment with Na<sub>2</sub>S in live cells. The cells were incubated with 5 μM of probe 1 for 30 min and then treated with different concentrations of Na<sub>2</sub>S at 37 °C for another 30 min. As shown in Fig. 5, the probe displayed negligible fluorescence (Fig. 5c). For the cells treated with Na<sub>2</sub>S, a significant fluorescence increase can be observed in the cytoplasm (Fig. 5f). In addition, increasing level of green fluorescence could be observed with increasing concentrations of Na<sub>2</sub>S (Fig. S8, Supporting Information). These experiments clearly showed that probe 1 can serve as a useful tool for monitoring the change of H<sub>2</sub>S levels in living cells.

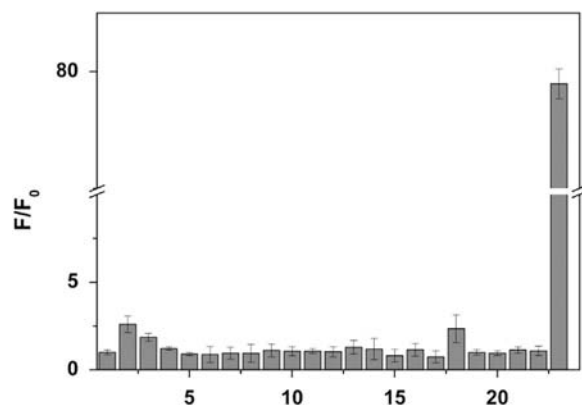


**Fig. 4.** Fluorescence responses of probe 1 (5 μM) after adding various ROS, RNS, RSS and other analytes and incubating at 37 °C for 60 min in Tris-HCl buffer (50 mM, pH=8.0, 50% DMF). The bars represent fluorescence response at 520 nm. (1) probe only; (2) cysteine; (3) GSH; (4) homocysteine; (5)  $\text{SO}_3^{2-}$ ; (6)  $\text{S}_2\text{O}_3^{2-}$ ; (7)  $\text{S}_2\text{O}_4^{2-}$ ; (8)  $\text{S}_2\text{O}_5^{2-}$ ; (9)  $\text{SCN}^-$ ; (10)  $\text{NO}_2^-$ ; (11)  $\text{NO}_3^-$ ; (12)  $\text{N}_3^-$ ; (13)  $\text{H}_2\text{O}_2$ ; (14)  $\text{HOCl}$ ; (15)  $\text{F}^-$ ; (16)  $\text{Cl}^-$ ; (17)  $\text{Br}^-$ ; (18)  $\text{I}^-$ ; (19)  $\text{HPO}_4^{2-}$ ; (20)  $\text{H}_2\text{PO}_4^-$ ; (21)  $\text{HCO}_3^-$ ; (22)  $\text{CO}_3^{2-}$ ; (23) Na<sub>2</sub>S. (the concentration of all the analyte is 1 mM except that of Na<sub>2</sub>S, which is 100 μM).

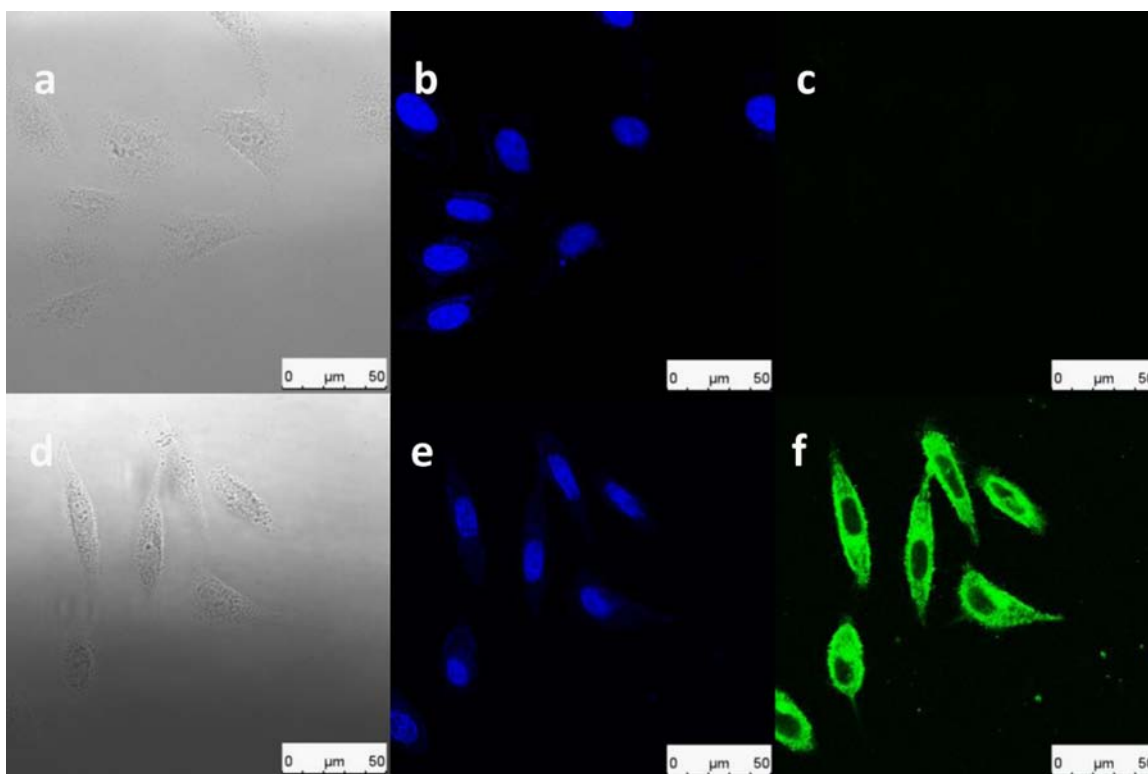


**Fig. 5.** Fluorescence images of  $\text{H}_2\text{S}$  with probe 1 in HeLa cells. HeLa cells were incubated with probe 1 ( $5 \mu\text{M}$ ) for 60 min. (a) Brightfield image, (b) Fluorescent image (using filters for Hoescht), (c) Fluorescent image (using filters for Fluorescein). HeLa cells were incubated with probe 1 for 30 min and then incubated with  $\text{Na}_2\text{S}$  ( $250 \mu\text{M}$ ) for another 30 min. (d) Brightfield image, (e) Fluorescent image (using filters for Hoescht), (f) Fluorescent image (using filters for Fluorescein). Scale bars represent  $50 \mu\text{m}$ .

#### 4. Conclusions

In conclusion, we have developed a new fluorescent probe based on iminocoumarin benzothiazole scaffold for detecting  $\text{H}_2\text{S}$ . The probe utilizes a  $\text{H}_2\text{S}$ -induced cascade reaction consisting of three consecutive steps: reduction, elimination and cyclization. Our studies show that the probe possesses high sensitivity and selectivity towards  $\text{H}_2\text{S}$ . Furthermore, the bioimaging experiments of  $\text{H}_2\text{S}$  prove that the probe can serve as a promising tool to further explore the biological roles of  $\text{H}_2\text{S}$  in complex biological environment.

#### Acknowledgments

The author would like to thank for the financial support from the City University of Hong Kong Grant (No. 9667091, 9610304), National Science Foundation of China (No. 21272212, 21390411), National Basic Research Program of China (No. 2011CB933101).

#### Appendix A. Supporting information

Supplementary data associated with this article can be found in the online version at <http://dx.doi.org/10.1016/j.talanta.2014.12.044>.

#### References

- [1] C. Szabo, *Nat. Rev. Drug Dis* 6 (2007) 917–935.
- [2] G. Yang, L. Wu, B. Jiang, W. Yang, J. Qi, K. Cao, Q. Meng, A.K. Mustafa, W. Mu, S. Zhang, S.H. Snyder, R. Wang, *Science* 322 (2008) 587–590.
- [3] L.F. Hu, M. Lu, Z.Y. Wu, P.T. Wong, J.S. Bian, *Mol. Pharmacol.* 75 (2009) 27–34.
- [4] K.H. Kulkarni, E.M. Monjok, R. Zeyssig, G. Kouamou, O.N. Bongmba, C.A. Opere, Y.F. Njie, S.E. Ohia, *Neurochem. Res.* 34 (2009) 400–406.
- [5] L. Li, M. Bhatia, P.K. Moore, *Curr. Opin. Pharmacol.* 6 (2006) 125–129.
- [6] A. Papapetropoulos, A. Pyriochou, Z. Altaany, G.D. Yang, A. Marazioti, Z.M. Zhou, M.G. Jeschke, L.K. Branski, D.N. Herndon, R. Wang, C. Szabo, *Proc. Natl. Acad. Sci. USA* 106 (2009) 21972–21977.
- [7] J.F. Wang, Y. Li, J.N. Song, H.G. Pang, *Neurochem. Int.* 64 (2014) 37–47.
- [8] M.H. Stipanuk, I. Ueki, *J. Inher. Metab. Dis.* 34 (2011) 17–32.
- [9] M. Whiteman, P.K. Moore, *J. Cell. Mole. Med.* 13 (2009) 488–507.
- [10] C.W. Leffler, H. Parfenova, J.H. Jaggard, R. Wang, *J. Appl. Physiol.* 100 (2006) 1065–1076.
- [11] L. Li, P. Rose, P.K. Moore, *Annu. Rev. Pharmacol. Toxicol.* 51 (2011) 169–187.
- [12] C. Jacob, E. Battaglia, T. Burkholz, D. Peng, D. Bagrel, M. Montenarh, *Chem. Res. Toxicol.* 25 (2012) 588–604.
- [13] P. Kamoun, M.C. Belardinelli, A. Chabli, K. Lallouchi, B. Chadefaux-Vekemans, *Am. J. Med. Genet. Part A* 116A (2003) 310–311.
- [14] W. Yang, G. Yang, X. Jia, L. Wu, R. Wang, *J. Physiol.* 569 (2005) 519–531.
- [15] S. Fiorucci, E. Antonelli, A. Mencarelli, S. Orlandi, B. Renga, G. Rizzo, E. Distrutti, V. Shah, A. Morelli, *Hepatology* 42 (2005) 539–548.
- [16] D. Jimenez, R. Martinez-Manez, F. Sancenon, J.V. Ros-Lis, A. Benito, J. Soto, *J. Am. Chem. Soc.* 125 (2003) 9000–9001.
- [17] N.S. Lawrence, J. Davis, R.G. Compton, *Talanta* 50 (2000) 771–784.
- [18] J. Wall, B. Chiswell, B. Hamilton, C. Dieckmann, K. O'Halloran, *Talanta* 45 (1997) 85–90.
- [19] N.S. Lawrence, J. Davis, L. Jiang, T.G.J. Jones, S.N. Davies, R.G. Compton, *Electroanalysis* 12 (2000) 1453–1460.
- [20] J. Radford-Knoery, G.A. Cutter, *Anal. Chem.* 65 (1993) 976–982.
- [21] P.R. Berube, P.D. Parkinson, E.R. Hall, *J. Chromatogr. A* 830 (1999) 485–489.
- [22] A.R. Lippert, E.J. New, C.J. Chang, *J. Am. Chem. Soc.* 133 (2011) 10078–10080.
- [23] H. Peng, Y. Cheng, C. Dai, A.L. King, B.L. Predmore, D.J. Lefler, B. Wang, *Angew. Chem. Int. Edit* 50 (2011) 9672–9675.
- [24] L.A. Montoya, M.D. Pluth, *Chem. Commun.* 48 (2012) 4767–4769.
- [25] S. Chen, Z.J. Chen, W. Ren, H.W. Ai, *J. Am. Chem. Soc.* 134 (2012) 9589–9592.
- [26] S.K. Das, C.S. Lim, S.Y. Yang, J.H. Han, B.R. Cho, *Chem. Commun.* 48 (2012) 8395–8397.
- [27] Q.Q. Wan, Y.C. Song, Z. Li, X.H. Gao, H.M. Ma, *Chem. Commun.* 49 (2013) 502–504.
- [28] Z. Wu, Z. Li, L. Yang, J. Han, S. Han, *Chem. Commun.* 48 (2012) 10120–10122.
- [29] C. Wei, Q. Zhu, W. Liu, W. Chen, Z. Xi, L. Yi, *Org. Biomol. Chem.* 12 (2014) 479–485.
- [30] Y. Jiang, Q. Wu, X.J. Chang, *Talanta* 121 (2014) 122–126.
- [31] C.R. Liu, J. Pan, S. Li, Y. Zhao, L.Y. Wu, C.E. Berkman, A.R. Whorton, M. Xian, *Angew. Chem. Int. Edit* 50 (2011) 10327–10329.
- [32] Z. Xu, L. Xu, J. Zhou, Y.F. Xu, W.P. Zhu, X.H. Qian, *Chem. Commun.* 48 (2012) 10871–10873.
- [33] Y. Qian, J. Karpus, O. Kabil, S.Y. Zhang, H.L. Zhu, R. Banerjee, J. Zhao, C. He, *Nat. Commun* 2 (2011) 495.

- [34] C. Liu, B. Peng, S. Li, C.M. Park, A.R. Whorton, M. Xian, *Org. Lett.* 14 (2012) 2184–2187.
- [35] K. Sasakura, K. Hanaoka, N. Shibuya, Y. Mikami, Y. Kimura, T. Komatsu, T. Ueno, T. Terai, H. Kimura, T. Nagano, *J. Am. Chem. Soc.* 133 (2011) 18003–18005.
- [36] F.P. Hou, J. Cheng, P.X. Xi, F.J. Chen, L. Huang, G.Q. Xie, Y.J. Shi, H.Y. Liu, D.C. Bai, Z.Z. Zeng, *Dalton Trans.* 41 (2012) 5799–5804.
- [37] D.Q. Zhang, W.S. Jin, *Spectrochim. Acta A* 90 (2012) 35–39.
- [38] T.I. Kim, H. Kim, Y. Choi, Y. Kim, *Chem. Commun.* 47 (2011) 9825–9827.
- [39] T.I. Kim, M.S. Jeong, S.J. Chung, Y. Kim, *Chem-Eur. J.* 16 (2010) 5297–5300.
- [40] Z.H. Liu, Q.L. Wang, L.Y. Mao, R.X. Cai, *Anal. Chim. Acta* 413 (2000) 167–173.
- [41] C.Y. Li, X.F. Kong, Y.F. Li, C. Weng, J.L. Tang, D. Liu, W.G. Zhu, *Anal. Chim. Acta* 824 (2014) 71–77.
- [42] A.L. Luo, Y.J. Gong, Y. Yuan, J. Zhang, C.C. Zhang, X.B. Zhang, W.H. Tan, *Talanta* 117 (2013) 326–332.
- [43] F. Yu, P. Li, P. Song, B. Wang, J. Zhao, K. Han, *Chem. Commun.* 48 (2012) 2852–2854.
- [44] F. Hou, L. Huang, P. Xi, J. Cheng, X. Zhao, G. Xie, Y. Shi, F. Cheng, X. Yao, D. Bai, Z. Zeng, *Inorg. Chem.* 51 (2012) 2454–2460.
- [45] G.J. Mao, T.T. Wei, X.X. Wang, S.Y. Huan, D.Q. Lu, J. Zhang, X.B. Zhang, W. Tan, G.L. Shen, R.Q. Yu, *Anal. Chem.* 85 (2013) 7875–7881.
- [46] W. Sun, J. Fan, C. Hu, J. Cao, H. Zhang, X. Xiong, J. Wang, S. Cui, S. Sun, X. Peng, *Chem. Commun.* 49 (2013) 3890–3892.
- [47] B. Chen, W. Li, C. Lv, M. Zhao, H. Jin, H. Jin, J. Du, L. Zhang, X. Tang, *Analyst* 138 (2013) 946–951.